Covid-19 Diagnosis by Gray-level Cooccurrence Matrix and Genetic Algorithm

Xiaoyan Jiang[1,*], Zuojin Hu[1], Mackenzie Brown[2], Hei-Ran Cheong[3]

[1]School of Mathematics Information Science, Nanjing Normal University of Special Education, Nanjing 210038, China
[2]School of Engineering, Edith Cowan University, Joondalup WA 6027, Australia
[3]Department Civil & Environment Engineering, University of Ulsan, Korea, Daehak Ro 93, Ulsan 680749, South Korea

Abstract

Currently, improving the identification of COVID-19 with the help of computer vision and artificial intelligence has received great attention from researchers. This paper proposes a novel method for automatic detection of COVID-19 based on chest CT to help radiologists improve the speed and reliability of tests for diagnosing COVID-19. Our algorithm is a hybrid approach based on the Gray-level Cooccurrence Matrix and Genetic Algorithm. The Gray-level Cooccurrence Matrix (GLCM) was used to extract CT scan image features, GA algorithm was used as an optimizer, and a feedforward neural network was used as a classifier. Finally, we use 296 chest CT scan images to evaluate the detection performance of our proposed method. To more accurately evaluate the accuracy of the algorithm, 10-run 10-fold cross-validation was introduced. Experimental results show that our proposed method outperforms state-of-the-art methods in terms of Sensitivity, Accuracy, F1, MCC, and FMI.

---

*Corresponding author. Email: j_njty@163.com

1. Introduction

Corona Virus Disease 2019 (COVID-19) is a serious and highly contagious disease caused by the novel coronavirus discovered in 2019 [1, 2]. As of May 17, 2022, there have been 519,729,804 confirmed cases of COVID-19 in the world and 6,268,281 deaths, according to the WHO real-time statistics. The number of confirmed cases and deaths continues to rise, the virus continues to mutate, and the global epidemic is far from over [3, 4].

According to the existing case data, Covid-19 is mainly manifested by fever, dry cough, fatigue, etc., and a small number of patients have upper respiratory and gastrointestinal symptoms such as nasal congestion, runny nose, and diarrhea [5-7]. Severe cases develop dyspnea, and more severe cases rapidly progress to acute respiratory distress syndrome [8], septic shock, difficult-to-correct metabolic acidosis, coagulation dysfunction, and multiple organ failure [9, 10].

It is self-evident that early detection, early diagnosis, and early treatment can significantly reduce the incidence and mortality of critical illness in patients with COVID-19 [11]. CT examination plays an important role in the diagnosis of COVID-19, and was once used as the main basis for clinical diagnosis in major epidemic areas [12]. However, conventional CT examination has some shortcomings, such as it is difficult to observe relatively hidden lesions in the early stage, and it is difficult to distinguish it from other viral pneumonia and bacterial pneumonia.

Deep learning [13-15] is a combination of machine learning methods whose algorithms specify features

through a series of non-linear functions that are organized in combination to maximize model accuracy. Deep learning mainly focuses on automatic feature extraction and classification of images. In healthcare, deep learning is used to efficiently generate models, resulting in more accurate results when using images to predict and classify different diseases without any human intervention.

Recently, deep learning methods have been widely applied to diagnose COVID-19 based on CT images, and studies have demonstrated that these methods can reliably extract feature information from chest CT images [16-18]. For example, Aseel Qassim Abdul Ameer et al. [19] designed a CT scan detection system for Covid-19 based on Gray-level Cooccurrence Matrix, which can detect the location of infection and detect whether the lungs are infected with 94% accuracy. Lu Xu et al. [20] developed three deep learning models, CNN, LSTM and CNN, to predict the number of COVID-19 cases, and successfully predicted the spread trend in Brazil, India, and Russia. Khabir Uddin Ahamed et al. [21] developed a deep learning-based COVID-19 case detection model trained on a dataset consisting of chest CT scans and X-ray images, helping radiologists use basic but widely available equipment to rapid diagnosis of COVID-19 cases. In [22], The authors focused on summarizing deep learning methods that have been significantly utilized in the automatic identification of COVID-19 cases from other lung diseases and normal populations while also discussing the challenges associated with current DL methods for COVID-19 diagnosis. For example, most datasets for binary or multi-class classification for COVID-19 diagnosis are highly unbalanced, medical images are often low-contrast image, etc.

In recent years, radial basis function neural network (RBFNN) [23], kernel-based extreme learning machine(K-ELM) [24], extreme learning machine with bat algorithm(ELM-BA) [25], etc. have been applied to COVID-19 detection. However, in the process of implementing the training algorithms of the classifiers, in the process of implementing the classifier training algorithm, they all face the situation of falling into local optimization or failing to achieve global optimization [26]. To solve the above issues, we propose a method to diagnose COVID-19 by using Gray-level Cooccurrence Matrix and Genetic Algorithm. This research is expected to help clinicians achieve more precise judgments in the diagnosis of COVID-19 patients.

In this study, the gray-level co-occurrence matrix is used to extract features from CT images of COVID-19 cases [27]. We use genetic algorithms to find optimal solutions, and cross-validation is used to test the performance of the algorithms[28].

The rest of this paper is organized as follows: In section 2, we briefly introduce the data sets of this research. In section 3, we first describe the basic concepts of the Gray-level Cooccurrence Matrix (GLCM) and its four typical statistical features. Next, the Feedforward Neural Network (FNN) and Genetic Algorithm (GA) is described, and K-fold cross-validation is given. In Section 4, we describe the experimental details and a discussion of the results. The conclusion of this research is described in Section 5.

2 Dataset

In our experiments, the dataset was divided into two subsets, 148 CT images of chest scans of patients diagnosed with COVID-19 and 148 CT images of chest scans of healthy subjects, for a total of 296 images. Among them, there were 66 COVID-19 patients (41 males and 25 females) and 66 healthy subjects (31 males and 35 females). These healthy subjects were randomly selected from the healthy population. In the experiments, we focused on the identification of COVID-19 by chest CT. For COVID-19 patients, the layer with the largest lesion characteristics was selected, while for healthy subjects, the image level was chosen arbitrarily. Figure 1 shows sample CT scan images of COVID-19 patients, and healthy controls, where (a) is a CT scan image sample of a COVID-19 patient and (b) is a CT scan image sample of healthy control (HC).
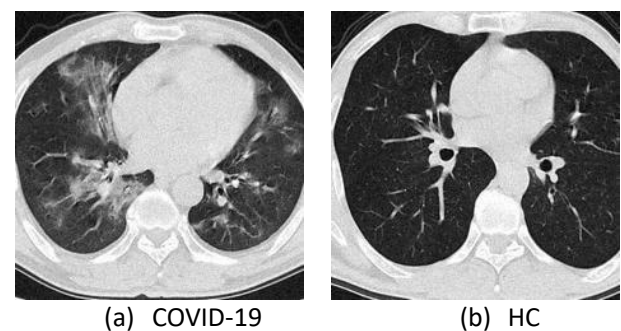

(a) COVID-19   (b) HC

Figure 1. Comparison of CT scan image samples of COVID-19 patients and healthy controls.

3 Methodology

3.1 GLCM

Gray-level Cooccurrence Matrix is a square matrix that can describe texture features by calculating the spatial correlation of image gray[29]. The GLCM texture considers the spatial relationship between two pixels at a specific orientation angle and distance, which reflects the two-dimensional statistical characteristics of image texture[30]. We must specify the offset value and direction as the gray-level co-occurrence matrix is constructed. When the offset value is 1, there are four directions: 0 °, 45 °, 90 ° and 135 °, and there is a gray-level co-occurrence matrix in each direction[29]. Then, the element value of the gray-level co-occurrence matrix is the number of times that the two gray values

represented by rows and columns in the image appear together in the specified direction and offset value.

There are 14 statistical characteristics of GLCM used to reflect the spatial correlation characteristics of images. Four of these characteristics are commonly correlated to texture, including energy, entropy, contrast, and homogeneity[31].

Energy (Equation (1)) [32] is the sum of squared of each element in the GLCM. *Energy* is a measure of the stability of the gray level change of the image texture, and reflects the uniformity of the image gray level distribution and the thickness of the texture.

$$Energy = \sum_{p,q} (C_a(p,q))^2 \tag{1}$$

Here, p and q are different element values of gray-level co-occurrence matrix, $C_a(p,q)$ represents the $(p,q)^{th}$ entry in a normalised grey-tone spatial dependence matrix which is the sum of the number of times that pixel value p was some distance and angle a from pixel intensity q.

Entropy (Equation (2)) is a measure of the randomness of the amount of information contained in an image. When all values in the co-occurrence matrix are equal, or the pixel values show the greatest randomness, the entropy is the largest. Therefore, *entropy* indicates the complexity of image gray distribution. The greater the entropy, the more complex the image is.

$$Entropy = \sum_{p,q} C_a(p,q) * log(C_a(p,q)) \tag{2}$$

Contrast (Equation (3))[30] reflects the contrast of the brightness between one pixel and its neighbor in relative location a.

$$Contrast = \sum_{p,q} |p-q|^2 C_a(p,q) \tag{3}$$

Homogeneity (Equation (4)) [32] compares the distribution of the values on the diagonal of the GLCM to the distribution of the values off the diagonal.

$$Homogeneity = \sum_{p,q} \frac{C_a(p,q)}{1+|p-q|} \tag{4}$$

3.2 Feedforward Neural Network

Feedforward neural network(FNN) is a directed acyclic graph that consists of input, hidden, and output neuron layers [33]. Layer 0, the layer that provides input Figure **2**[41]. In the figure, t refers to the evolutionary algebra counter.

variables to the network is called the input layer, the last layer is called the output layer, and other intermediate layers are considered hidden layers. In this neural network [34-36], each layer contains several neurons that can receive the signal of the previous layer of neurons and produce output to the next layer [26]. Any two nodes of two adjacent layers are connected. In other words, layers are fully connected.

In a feedforward neural network, the output of each neuron in the upper layer is used as input, and the output of this node is obtained through linear transformation (combined with bias) and non-linear function activation and is passed to the node in the next layer. The activation function gives the neural network the ability to "piecewise function" and can approximate any function. Without an activation function, a neural network is just a linear function and cannot solve any non-linear problems. *ReLU* is an activation function commonly used in artificial neural networks (Equation (5)) [33].

$$ReLU(m) = \begin{cases} m & m \geq 0 \\ 0 & m < 0 \end{cases} \tag{5}$$
$$= max(0, m)$$

Here, m is the input variable. When FNN is trained, it is necessary to find the most appropriate parameter weights and biases to best approximate the data. Usually, a loss function is designed to measure the approximation effect, and the optimal parameters should minimize the loss function. The cross-entropy loss function is the most commonly used in classification problems [37-39].

3.3 Genetic Algorithm

A genetic Algorithm (GA) is a computational model that simulates the natural selection and genetic mechanism of Darwin's theory of biological evolution, and it is a method to search for optimal solutions by simulating the natural evolution process [40]. The genetic algorithm does not directly deal with the decision variables of the solution space, but converts them into chromosomes composed of genes according to a certain structure through coding. The typical steps of genetic algorithm are: initialization, selection operation, crossover operation, mutation operation and termination condition judgment. The basic operation process of a typical genetic algorithm is shown in
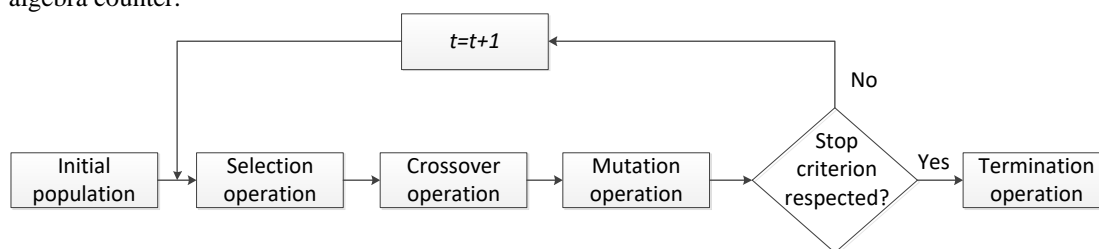

Figure 2. Diagram of a genetic algorithm.

3.3.1. Initial population

The process starts with a group of individuals called a population, each of which is a proposed solution to a defined problem. Individuals are also called chromosomes. A chromosome consists of a certain number of genes. The smallest taxonomic unit in the genetic algorithm is a gene. The generation of the initial population is random [42, 43]. Before the initial population is assigned, try to make a rough interval estimation to avoid the initial population being distributed in the coding space far from the optimal solution, which will limit the search range of the genetic algorithm. If the size of the group is set too small [44, 45], it may lead to premature convergence, and eventually the global optimal solution cannot be obtained; and if the size of the group is set too large, it will affect the calculation time. Therefore, the size of the population should be determined according to the actual problem. In the initial stage, the evolutionary algebra counter t is set to 0, and the maximum evolutionary algebra is set.

3.3.2. Selection operation

In this step, individuals who are more adapted to the environment need to be selected from the population. The purpose is to directly inherit the optimized individuals to the next generation or to generate new individuals through pairing and crossover to the next generation, so this operation is also called regeneration. The selection operation is based on the fitness evaluation of individuals in the group, that is, the probability of an individual being selected is related to the fitness value. The higher the individual fitness value, the greater the probability of being selected .

In genetic algorithm, roulette wheel selection and elitism selection are two typical selection methods. Taking the roulette wheel selection as an example, assuming that the size of the current population is M, and the fitness of individual i is f_i , the probability P_i (Equation (6))of individual i being selected is:

$$P_i = \frac{f_i}{\sum_{n=1}^{M} f_n} \tag{6}$$

Here, the denominator refers to the total fitness of the population.

3.3.3. Crossover operation

In the crossover operation, two individuals are randomly selected from the population, and through the exchange and combination of two chromosomes, the excellent characteristics of the parent string are inherited to the substring, thereby generating new excellent individuals.

3.3.4. Mutation operation

In the search process, in order to maintain the diversity of the population and prevent the genetic algorithm from prematurely converging in the optimization process and falling into a local optimal solution, it is necessary to mutate the individual, thereby changing the initial value of one or more genes in the chromosome [46, 47]. In practical applications, single-point mutation, also known as bit mutation, is mainly used, that is, only a certain bit in the gene sequence needs to be mutated. Take binary coding as an example, that is, 0 becomes 1, and 1 becomes 0.

3.3.5. Termination operation

When the fitness of the optimal individual reaches a given threshold, or the fitness of the optimal individual and the fitness of the group no longer rise, or the number of iterations reaches a preset number of generations, the algorithm terminates. Otherwise, replace the previous generation population with the new generation population obtained through selection, crossover, and mutation, and return to the selection operation to continue the loop execution.

3.4 K-fold cross validation

In the case of insufficient sample size, in order to make full use of the data set to test the effect of the algorithm, cross validation is introduced. Cross validation is a commonly used method when building models and validating model parameters in machine learning. In K-fold cross validation, a given data set is chunked into K parts in equal proportions, and one of them is used as test data, and the other K-1 data is used as training data. Afterward, K experiments were operated. In each experiment, a different data part is selected from the K parts as the test data, and the remaining K-1 parts are used as the training data, and the corresponding error rate is obtained. Finally, the error rate of the obtained K experimental results is averaged, so as to estimate the accuracy of the algorithm. **Figure 3** below shows the sequence of these operations. In K-fold cross validation, it should be noted that the data of K parts must be tested separately.
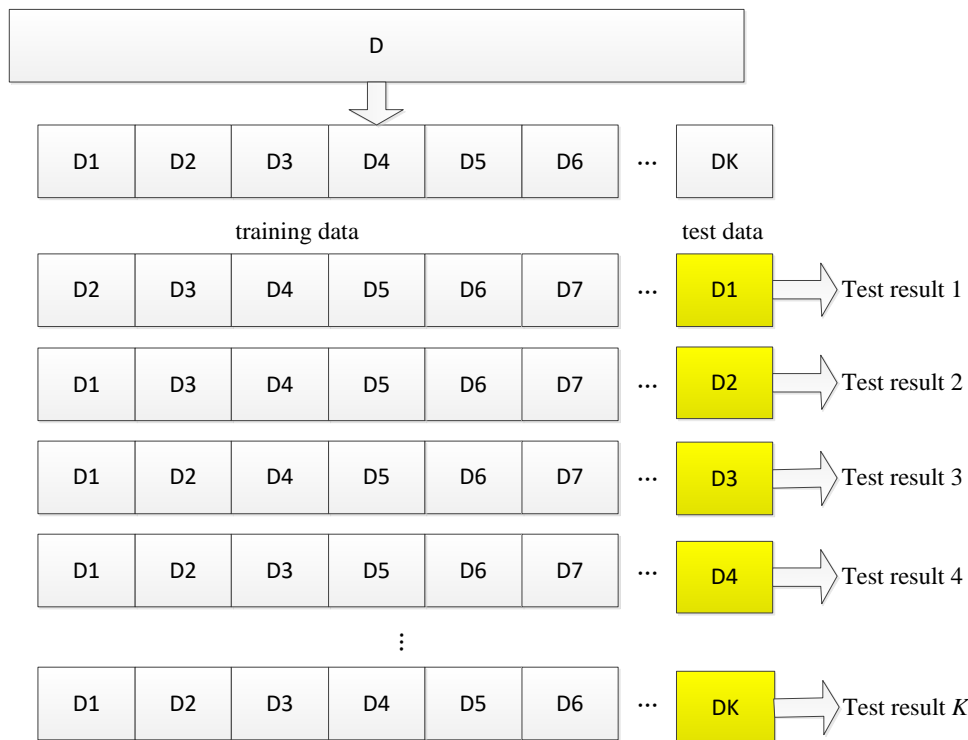
Figure 3. The main process of K-fold cross-validation.

$$E = \frac{1}{K} \sum_{i=1}^{K} E_i \qquad (7)$$

In Equation (7), i is the number of folds (i loops from 1 to K), E_i is the ith misclassification rate, and E is the average of K misclassification rates.

There may be bias or variance in the cross-validation. If K is increased, the variance will go up but the bias may go down [48-50]. Conversely, K is lowered, the bias may rise but the variance will fall. In general, the value of K depends on the situation of different projects. Of course, there must be K is less than the number of data pieces whose the training set [51].

4 Experiment Results and Discussions

4.1 GLCM Results

In the study, GLCM extracts the texture features of CT images from four directions (0°, 45°, 90° and 135°), and generates four matrices for each image. When the distance between the current pixel and its neighbor is set to 1, the angle can be set.

•Offset=[0 1]: GLCM at 0 °.

•Offset=[-1 1]: GLCM at 45 °.

•Offset=[-1 0]: GLCM at 90 °.

•Offset=[-1 -1]: GLCM at 135 °.

	1	2	3	4	5	6
1	3764	1149	73	15	2	0
2	1137	10196	1183	134	34	4
3	83	1177	2108	626	165	16
4	14	153	640	1068	495	82
5	2	43	152	548	8047	2653
6	0	5	19	61	2686	12768

(a) Offset=[0 1]

	1	2	3	4	5	6
1	3284	1254	144	78	60	8
2	1317	9671	1276	190	140	60
3	140	1297	1839	641	178	75
4	79	233	618	902	488	125
5	64	149	212	517	7124	3374
6	14	45	71	111	3429	11869

(b) Offset =[-1 1]

	1	2	3	4	5	6
1	3546	1112	135	66	35	0
2	1188	10091	1094	172	135	32
3	143	1137	2113	541	180	62
4	66	190	557	1085	450	100
5	25	121	199	467	7776	2886
6	0	21	68	111	2893	12505

(c) Offset=[-1 0]

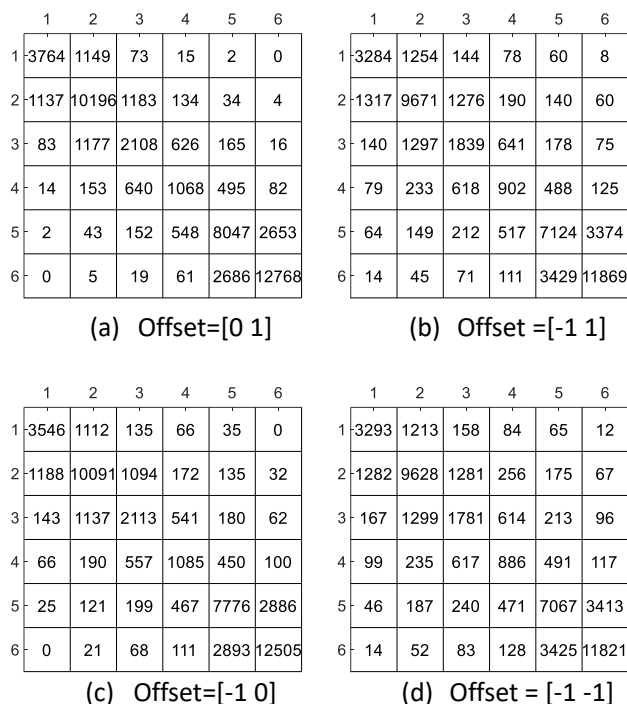|	1	2	3	4	5	6
1	3293	1213	158	84	65	12
2	1282	9628	1281	256	175	67
3	167	1299	1781	614	213	96
4	99	235	617	886	491	117
5	46	187	240	471	7067	3413
6	14	52	83	128	3425	11821

(d) Offset = [-1 -1]

Figure 4. GLCM values in four different directions.

In the experiment, four 6×6 gray-level co-occurrence matrixes in different directions are generated according to Figure 1(a), as shown in Figure 4. we use the obtained matrix to calculate features. Each gray-level co-occurrence matrix can be described 4 features: energy, entropy, contrast and homogeneity, and a total of 16 features are obtained and sent to the feedforward neural network.

4.2 Statistical Results

In the experiments, 10-Fold CV is introduced, meanwhile to more accurately evaluate the accuracy of the algorithm, we run 10-Fold CV 10 times. We evaluated the algorithm proposed in this study through 7 evaluation indicators: Sensitivity, Specificity, Precision, Accuracy, F1, Matthew's Correlation Coefficient (MCC), and Fowlkes–Mallows index(FMI). Here, F1 refers to F1-score, which is used as an evaluation standard to measure the comprehensive performance of the classifier [26]. The evaluation results are shown in

Table 1. It can be seen from the evaluation results that the performance of these metrics is significantly better than that of traditional methods.

Table 1. Statistics of experimental results.

Run	Sensitivity	Specificity	Precision	Accuracy	F1	MCC	FMI
1	75.68	72.30	73.20	73.99	74.42	48.00	74.43
2	68.24	76.35	74.26	72.30	71.13	44.74	71.19
3	71.62	71.62	71.62	71.62	71.62	43.24	71.62
4	75.68	71.62	72.73	73.65	74.17	47.34	74.19
5	78.38	70.27	72.50	74.32	75.32	48.81	75.38
6	74.32	74.32	74.32	74.32	74.32	48.65	74.32
7	77.70	70.27	72.33	73.99	74.92	48.11	74.97
8	77.70	68.24	70.99	72.97	74.19	46.15	74.27
9	74.32	73.65	73.83	73.99	74.07	47.97	74.07
10	68.92	74.32	72.86	71.62	70.83	43.31	70.86
MSD	74.26	72.30	72.86	73.28	73.50	46.63	73.53
	±3.60	±2.40	±1.09	±1.07	±1.65	±2.15	±1.65

4.3 Comparison to State-of-the-art Approaches

To test the effect of our proposed method, we used the ten-fold cross-validation method to verify it. Then we compared our GLCM-GA method with state-of-the-art methods: RBFNN, K-ELM, and ELM-BA. As shown in Table 2 and
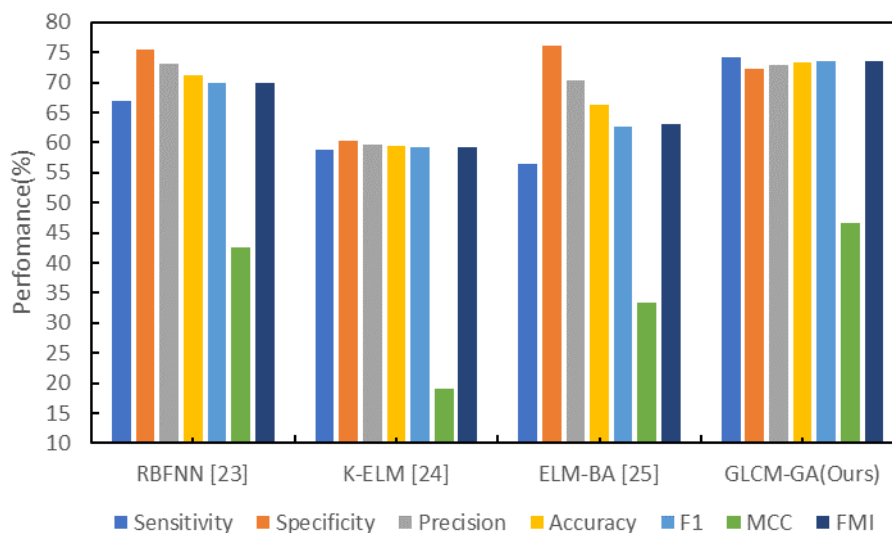

Figure 5, in terms of Sensitivity, Accuracy, F1, MCC, and FMI for detecting COVID-19, the best is GLCM-GA (Ours), followed by RBFNN, the third is ELM-BA, and the last is K-ELM. In the detection of Sensitivity for COVID-19, the best is GLCM-GA (Ours),

followed by RBFNN, the third is K-ELM, and the last is ELM-BA. In the Precision tests for COVID-19, the best is RBFNN, followed by GLCM-GA (Ours), the third is ELM-BA, and the last is K-ELM. In the Specificity tests for COVID-19, the best is RBFNN, followed by ELM-BA, the third is GLCM-GA (Ours), and the last is K-ELM.

Through the above analysis, it is found that the method of GLCM-GA (Ours) proposed by us had the best performance among the five detection indicators of COVID-19, although it is slightly lower than other methods in terms of specificity and precision.

Table 2. Comparison with state-of-the-art methods for detecting COVID-19.

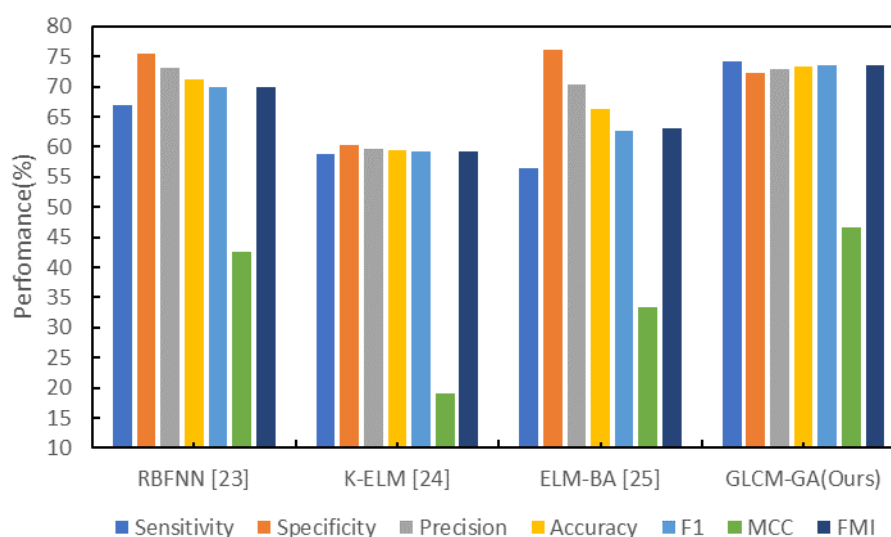| Method	Sensitivity	Specificity	Precision	Accuracy	F1	MCC	FMI
RBFNN [23]	66.89 ±2.43	75.47 ±2.53	73.23 ±1.48	71.18 ±0.80	69.88 ±1.08	42.56 ±1.61	69.97 ±1.04
K-ELM [24]	58.78 ±3.36	60.27 ±3.89	59.73 ±1.68	59.53 ±1.42	59.19 ±1.86	19.09 ±2.83	59.22 ±1.79
ELM-BA [25]	56.55 ±2.99	76.22 ±2.56	70.45 ±1.61	66.39 ±1.05	62.69 ±1.76	33.46 ±2.07	63.09 ±1.60
GLCM-GA (Ours)	74.26 ±3.60	72.30 ±2.40	72.86 ±1.09	73.28 ±1.07	73.50 ±1.65	46.63 ±2.15	73.53 ±1.65

Figure 5. Bar plot of comparison results.

5 Conclusions

In this study, we propose a hybrid diagnosis method based on the Gray-level Cooccurrence Matrix and Genetic Algorithm for COVID-19. The method consists of three parts: GLCM as feature extractor, FNN as classifier, and GA algorithm as optimizer. In the experiment, 10-run 10-fold cross validation was introduced. Compared with the existing global optimization methods (See Section 4.3), the GLCM-GA method proposed in this paper has better performance than other methods in terms of Sensitivity, Accuracy, F1, MCC and FMI.

The proposed method still has some shortcomings that need to be improved. For example, our method is not optimal in terms of specificity and accuracy, and we will improve the GLCM-GA method. Moreover, the dataset used in the experiment is small, containing only 296 images, so we will expand the dataset to test our method by acquiring multiple CT scan images.

In future work, we will attempt to combine other deep learning algorithms to improve the reliability of automatic diagnosis of COVID-19. In the future, we will also differentiate between COVID-19 and other viral diseases, such as common pneumonia, based on computer vision and deep learning.

References

[1] Wubet, G.K., Value chain analysis of Garlic in LiboKemkem District: In the era of COVID-19, South Gondar Zone Amhara Region, Ethiopia. Cogent Business & Management, 2022. **9**(1).

[2] Klasen, J.M., et al., Medical students' perceptions of learning and working on the COVID-19 frontlines: ' horizontal ellipsis a confirmation that I am in the right place professionally'. Medical Education Online, 2022. **27**(1).

[3] Yang, L., EDNC: ensemble deep neural network for Covid-19 recognition. Tomography, 2022. **8**(2): p. 869-890.

[4] Zhang, X., Diagnosis of COVID-19 pneumonia via a novel deep learning architecture. Journal of Computer Science and Technology, 2022. **37**(2): p. 330-343.

[5] Jiang, F., et al., Review of the Clinical Characteristics of Coronavirus Disease 2019 (COVID-19). Journal of General Internal Medicine, 2020. **35**(5): p. 1545-1549.

[6] Xu, X.W., et al., Clinical findings in a group of patients infected with the 2019 novel coronavirus (SARS-Cov-2) outside of Wuhan, China: Retrospective case series. BMJ (online), 2020. **368**: p. m606.

[7] Chen, W., et al., A novel coronavirus outbreak of global health concern. Lancet (London, England). **395**(10223): p. 470-473.

[8] Shih, E., et al., Treatment of acute respiratory distress syndrome from COVID-19 with extracorporeal membrane oxygenation in obstetrical patients. American Journal of Obstetrics & Gynecology MFM, 2022. **4**(2): p. 100537.

[9] Yang, X., et al., Clinical course and outcomes of critically ill patients with SARS-CoV-2 pneumonia in Wuhan, China: a single-centered, retrospective, observational study. The Lancet Respiratory Medicine, 2020. **8**(5): p. 475-481.

[10] Llitjos, J.F., et al., High incidence of venous thromboembolic events in anticoagulated severe COVID-19 patients. Journal of Thrombosis and Haemostasis, 2020. **18**.

[11] Tianjin, C.A.o., W.D.G. Hospital, and W.T.D. Hospital, Handbook of Prevention and Treatment of the Pneumonia Caused by the Novel Coronavirus (2019-nCoV). 2020.

[12] Wang, J., et al., CT characteristics of patients infected with 2019 novel coronavirus: association with clinical type. Clinical Radiology, 2020. **75**(6): p. 408-414.

[13] Dos Santos, C.F.G., et al., Gait Recognition Based on Deep Learning: A Survey. Acm Computing Surveys, 2023. **55**(2).

[14] Gafoor, S.A., et al., Deep learning model for detection of COVID-19 utilizing the chest X-ray images. Cogent Engineering, 2022. **9**(1).

[15] Lim, Y.W., A.S. Adler, and D.S. Johnson, Predicting antibody binders and generating synthetic antibodies using deep learning. Mabs, 2022. **14**(1).

[16] Hassan, H., et al., Supervised and weakly supervised deep learning models for COVID-19 CT diagnosis: A systematic review. Computer Methods and Programs in Biomedicine, 2022. **218**: p. 106731.

[17] Desai, S.B., A. Pareek, and M.P. Lungren, Deep learning and its role in COVID-19 medical imaging. Intelligence-Based Medicine, 2020. **3-4**: p. 100013.

[18] Aishwarya, T. and V.R. Kumar, Machine Learning and Deep Learning Approaches to Analyze and Detect COVID-19: A Review. SN Computer Science, 2021. **2**(3).

[19] Ameer, A.Q.A. and R.F. Mohammed, Covid-19 detection using CT scan based on gray level Co-Occurrence matrix. Materials Today: Proceedings, 2021.

[20] Xu, L., R. Magar, and A. Barati Farimani, Forecasting COVID-19 new cases using deep learning methods. Computers in Biology and Medicine, 2022. **144**: p. 105342.

[21] Ahamed, K.U., et al., A deep learning approach using effective preprocessing techniques to detect COVID-19 from chest CT-scan and X-ray images. Computers in Biology and Medicine, 2021. **139**: p. 105014.

[22] Aggarwal, P., et al., COVID-19 image classification using deep learning: Advances, challenges and opportunities. Computers in Biology and Medicine, 2022. **144**: p. 105350.

[23] Lu, Z., A Pathological Brain Detection System Based on Radial Basis Function Neural Network. Journal of Medical Imaging and Health Informatics, 2016. **6**(5): p. 1218-1222.

[24] Yang, J., A pathological brain detection system based on kernel based ELM. Multimedia Tools and Applications, 2018. **77**(3): p. 3715-3728.

[25] Lu, S., A Pathological Brain Detection System based on Extreme Learning Machine Optimized by Bat Algorithm. CNS & Neurological Disorders - Drug Targets, 2017. **16**(1): p. 23-29.

[26] Wang, S., et al., Diagnosis of COVID-19 by Wavelet Renyi Entropy and Three-Segment Biogeography-Based Optimization. International Journal of Computational Intelligence Systems, 2020. **13**(1): p. 1332-1344.

[27] Pi, P. and D. Lima, Gray level co-occurrence matrix and extreme learning machine for Covid-19 diagnosis. International Journal of Cognitive Computing in Engineering, 2021. **2**: p. 93-103.

[28] Acosta-González, E., J. Andrada-Félix, and F. Fernández-Rodríguez, On the evolution of the COVID-19 epidemiological parameters using only the series of deceased. A study of the Spanish outbreak using Genetic Algorithms. Mathematics and Computers in Simulation, 2022. **197**: p. 91-104.

[29] Santoni, M.M., et al., Cattle Race Classification Using Gray Level Co-occurrence Matrix Convolutional Neural Networks. Procedia Computer Science, 2015. **59**: p. 493-502.

[30] Srivastava, D., et al., Pattern-based image retrieval using GLCM. Neural Computing and Applications, 2020. **32**(8): p. 1-14.

[31] Akkoç, B., A. Arslan, and H. Kök, Gray level co-occurrence and random forest algorithm-based gender determination with maxillary tooth plaster images. Computers in Biology and Medicine, 2016. **73**: p. 102-107.

[32] Ossai, C.I. and N. Wickramasinghe, GLCM and statistical features extraction technique with Extra-Tree Classifier in Macular Oedema risk diagnosis. Biomedical Signal Processing and Control, 2022. **73**: p. 103471.

[33] Li, D., et al., Intelligent rockburst prediction model with sample category balance using feedforward neural network and Bayesian optimization. Underground Space, 2022.

[34] Satapathy, S.C., Fruit category classification by fractional Fourier entropy with rotation angle vector grid and stacked sparse autoencoder. Expert Systems, 2022. **39**(3).

[35] Satapathy, S.C., Secondary pulmonary tuberculosis identification via pseudo-Zernike moment and deep stacked sparse autoencoder. Journal of Grid Computing, 2022. **20**.

[36] Karaca, Y., Secondary pulmonary tuberculosis recognition by rotation angle vector grid-based fractional Fourier entropy. Fractals, 2022. **30**(1).

[37] Govindaraj, V., Deep Rank-Based Average Pooling Network for Covid-19 Recognition. Computers, Materials & Continua, 2022. **70**: p. 2797-2813.

[38] Khan, M.A., VISPNN: VGG-Inspired Stochastic Pooling Neural Network. Computers, Materials & Continua, 2022. **70**: p. 3081-3097.

[39] Wang, S.-H., DSSAE: Deep Stacked Sparse Autoencoder Analytical Model for COVID-19 Diagnosis by Fractional Fourier Entropy. ACM Transactions on Management Information Systems, 2021. **13**(1).

[40] Estran, R., A. Souchaud, and D. Abitbol, Using a genetic algorithm to optimize an expert credit rating model. Expert Systems with Applications, 2022. **203**: p. 117506.

[41] Alfarizi, M.G., M. Stanko, and T. Bikmukhametov, Well control optimization in waterflooding using genetic algorithm coupled with Artificial Neural Networks. Upstream Oil and Gas Technology, 2022. **9**: p. 100071.

[42] Li, J., Texture Analysis Method Based on Fractional Fourier Entropy and Fitness-scaling Adaptive Genetic Algorithm for Detecting Left-sided and Right-sided Sensorineural Hearing Loss. Fundamenta Informaticae, 2017. **151**(1-4): p. 505-521.

[43] Hou, X.-X., Alcoholism detection by medical robots based on Hu moment invariants and predator-prey adaptive-inertia chaotic particle swarm optimization. Computers and Electrical Engineering, 2017. **63**: p. 126-138.

[44] Singh, V.K., et al., Novel Genetic Algorithm (GA) based hybrid machine learning-pedotransfer Function (ML-PTF) for prediction of spatial pattern of saturated hydraulic conductivity. Engineering Applications of Computational Fluid Mechanics, 2022. **16**(1): p. 1082-1099.

[45] Almuzaini, H.A. and A.M. Azmi, An unsupervised annotation of Arabic texts using multi-label topic modeling and genetic algorithm. Expert Systems with Applications, 2022. **203**.

[46] Boukhobza, A., et al., Design of orthogonal filter banks using a multi-objective genetic algorithm for a speech coding scheme. Alexandria Engineering Journal, 2022. **61**(10): p. 7649-7657.

[47] Kyriklidis, C., et al., Optimal Bio Marine Fuel production evolutionary Computation: Genetic algorithm approach for raw materials mixtures. Fuel, 2022. **323**.

[48] Khan, M.A., Pseudo Zernike Moment and Deep Stacked Sparse Autoencoder for COVID-19 Diagnosis. CMC-Computers, Materials & Continua, 2021. **69**(3): p. 3145–3162.

[49] Jiang, X., Multiple Sclerosis Recognition by Biorthogonal Wavelet Features and Fitness-Scaled Adaptive Genetic Algorithm. Frontiers in Neuroscience, 2021. **15**(1098).

[50] Zhang, Z. and X. Zhang, MIDCAN: A multiple input deep convolutional attention network for Covid-19 diagnosis based on chest CT and chest X-ray. Pattern Recognition Letters, 2021. **150**: p. 8-16.

[51] Lyu, Z., et al., Back-Propagation Neural Network Optimized by K-Fold Cross-Validation for Prediction of Torsional Strength of Reinforced Concrete Beam. Materials, 2022. **15**(4): p. 1477.